Organic LETTERS

Letter

pubs.acs.org/OrgLett

Development of Solid-State Emissive Materials Based on Multifunctional *o*-Carborane–Pyrene Dyads

Kenta Nishino, Hideki Yamamoto, Kazuo Tanaka,* and Yoshiki Chujo*

Department of Polymer Chemistry, Graduate School of Engineering, Kyoto University Katsura, Nishikyo-ku, Kyoto 615-8510, Japan

Supporting Information

ABSTRACT: The molecular design based on *o*-carborane dyads is described for preparing multifunctional luminescent molecules such as dual emissions, aggregation and crystallization-induced emission enhancements, and luminescent color changes. The pyrene-substituted *o*-carborane dyads were synthesized via the insertion reaction between decaborane and 1-ethynylpyrene in the presence of Lewis base in a good yield. Finally, extremely bright luminescent compounds with solid-state emission properties (Φ_{PL} > 0.99) were obtained.

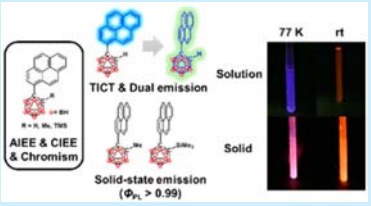

Solid-state emissive compounds composed of conjugated molecules have attracted much attention as a versatile platform for realizing advanced optically functional materials and organic light-emitting devices. To receive highly functional devices, the development of key building blocks which can induce solid-state emission is a topic with high relevance. One of the crucial difficulties to be solved in the development of solid-state emissive molecules is aggregation-caused quenching (ACQ) which is generally observed as a critical annihilation process in the condensed state. Contrary to conventional organic dyes showing ACQ, it was found that some classes of organic dyes[1] and recently organoboron complexes[2] can present bright emission only in the aggregation state. These phenomena are called aggregation-induced emission (AIE) or AIE enhancement (AIEE). Since the application of solid-state emission from AIE-active molecules to the material design should be a valid strategy to overcome ACQ, new AIE-active molecules and comprehension of photochemical mechanism for their emissions are of great significance to receive highly efficient solid-state emissive materials.[3]

o-Carborane is a class of boron cluster compounds composed of two carbon and ten boron atoms (1,2-dicarba-*closo*-dodecaborane) and has been focused as an optically functional "element-block"[4] which is defined as a functional heteroatom-containing building block.[5] In particular, since the first report on the AIE-active *o*-carborane polymers, *o*-carborane is recognized as an AIE-inducible "element block".[6] *o*-Carborane works as an electron-withdrawing group because of the electron-deficient characteristics of skeletal electrons delocalized via the 3-center-2-electron bonds.[7] Therefore, by combination with the electron-donating groups or aromatic units, robust electronic conjugation can be constructed via the σ^*–π^* conjugation, leading to large emission bands from the intramolecular charge transfer (ICT) transition.[8] The vibration at the C–C bond in *o*-carborane consumed excitation energy, resulting in the annihilation in the solution state.[6a] In contrast, strong emission can be recovered in the solid state by suppressing this intramolecular motion. Thus, AIE properties can be obtained. Moreover, it was proposed that the degree of donor–acceptor interaction should be significantly enhanced at the perpendicular conformation between the C–C bond in *o*-carborane and the conjugated plane involving the directly connected aromatic unit to *o*-carborane.[9] It can be said that such structural anisotropy should be unique characteristics of *o*-carborane-based electronic acceptors.

Herein, we report the molecular design based on *o*-carborane dyads for preparing multifunctional luminescent molecules such as dual emissions, AIEE, crystallization-induced emission enhancement (CIEE), luminescent chromism, and highly efficient solid-state emissions. Initially, the pyrene-substituted *o*-carborane dyad was synthesized, and dual emissions were observed in the solution state. It was revealed that these emissions were assigned as locally excited (LE) and ICT emission bands. Additionally, it was clarified that the dyad had an AIEE property attributable to the ICT emission band. Furthermore, in the aggregation and crystalline states, large emission efficiencies were obtained (Φ_{PL} = 0.40 and 0.80, respectively). It was suggested that the rotation at the carborane moiety could occur even in the solid state, leading to the twisted intramolecular charge transfer (TICT) emission.[10] On the basis of this speculation, to confirm the TICT mechanism and to improve the solid-state emissive abilities by completely suppressing molecular motions, the methyl and TMS-substituted carborane dyads were prepared. Finally, extremely bright luminescent compounds with solid-state emission properties (Φ_{PL} > 0.99) were obtained. This manuscript presents the feasible "element block" as an optically multifunctional unit based on *o*-carborane.

The synthesis of *o*-carborane dyads was performed according to Scheme 1. 1-(Trimethylsilyl)ethnylpyrene was obtained from 1-bromopyrene through the Sonogashira–Hagihara coupling reaction with $PdCl_2(PPh_3)_2$ as a catalyst. Then the trimethylsilyl (TMS) group was removed in the presence of tetrabutylammonium fluoride. Finally, **CBP-H** having orange

Received: July 5, 2016
Published: July 29, 2016

ACS Publications © 2016 American Chemical Society

DOI: 10.1021/acs.orglett.6b01920
Org. Lett. 2016, 18, 4064–4067

Scheme 1. Synthesis of *o*-Carborane–Pyrene Dyads

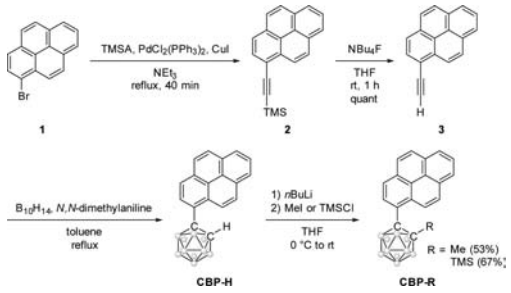

emission was obtained by the insertion reaction of 1-ethynylpyrene into decaborane (Figure S21). By introducing methyl and TMS groups at another carbon in *o*-carborane, **CBP-Me** and **CBP-TMS** possessing green and yellow emissions were obtained, respectively (Figures S22 and S23). The product was characterized by ^{1}H, ^{11}B, and ^{13}C NMR and mass measurements and an elemental analysis. The product showed good stability toward air and light under ambient conditions. From these data, we concluded that the product possessed the designed structure and stability high enough for the optical measurements.

Initially, optical properties were evaluated in the diluted solution for examining the intrinsic electronic properties of the dyad. Figure 1a shows the photoluminescence (PL) spectra of

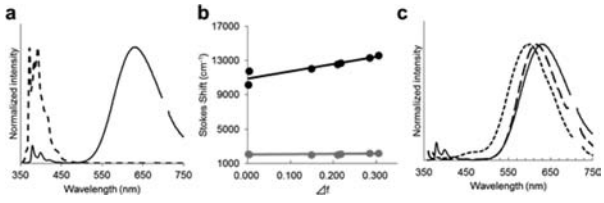

Figure 1. (a) PL spectra of pyrene (dashed line) and **CBP-H** (solid line). All samples were measured in THF (1.0×10^{-5} M) and excited at 351 nm. All spectra were normalized at λ_{max}. (b) Lippert–Mataga plots of **CBP-H**. Gray and black dots represent emission peaks in shorter and longer wavelength regions, respectively. (c) PL spectra of **CBP-H** in the THF solution (solid line), water suspension (dotted line), and crystalline state (dashed line).

CBP-H and pyrene as the model compound in THF. Pyrene showed the vibrational emission peaks around 400 nm. Correspondingly, **CBP-H** also presented a similar spectral pattern around the same region. Interestingly, the broad emission band with a peak around 600 nm was obtained. The emission intensity of this broad emission band in the longer wavelength region was much larger than that in the shorter wavelength region. According to the kinetic data as listed in Table S2, these emissions should be fluorescent. Moreover, phosphorescence was hardly observed from any compounds.

To investigate the emission mechanism from **CBP-H**, the changes in absorption and PL spectra were monitored with variable solvents such as hexane, benzene, dichloromethane, chloroform, acetone, and acetonitrile (Figures S10 and S11). Significant peak shifts were hardly observed in the absorption spectra. In contrast, drastic peak shifts were shown from the broad emission band in the longer wavelength region in the PL spectra. By increasing solvent polarity, red-shifted emissions were obtained. To analyze the solvatochromic luminescence, the Lippert–Mataga plots were prepared with the values of the Stokes shift against the solvent polarizability, Δf, according to the eq (Figure 1b).[11] It was indicated that the slope of the approximate line prepared from the emission band around 400 nm was almost zero. On the other hand, the significant keen slope was obtained from the plots with the peak positions observed around 600 nm. These data indicate that the luminescent bands around 400 and 600 nm should be assigned to the LE state of the pyrene moiety and the ICT state, respectively. Usually, the emission band from the LE state can be observed only under frozen or structurally restricted environmental conditions.[12] The intramolecular rotation could be disturbed even in the solution state. Additionally, the transition dipole moment was estimated as 10.73 D according to the Lippert–Mataga equation. This value is relatively larger than those of previous luminescent dyes with ICT emission properties.[11] It is suggested that structural alteration could proceed in the excited state.

To examine the possibility of the structural alteration during the ICT process, PL spectra were monitored with variable temperatures from 10 to 50 °C (Figure S12). Accordingly, it was indicated that the ratios between the magnitude of the CT emission and that of the LE emission increased by increasing the detection temperature. This behavior was often observed in the emission from the TICT mechanism.[13] Furthermore, from the PL spectrum recorded at 77 K, only the LE emission was obtained (Figure S13). These data strongly support that the dual-emission properties of **CBP-H** should be from the LE and TICT states.

To estimate the relationship between the dihedral angle which is defined as the directional difference between the C–C bond in the *o*-carborane moiety and the pyrene group and optical properties, quantum calculation was performed by using density functional theory (DFT) and time-dependent DFT (TD-DFT). As mentioned in the introduction, the degree of electronic interaction should be enhanced in the perpendicular conformation between the C–C bond in the *o*-carborane moiety and the aryl group. On this basis, electronic structures were investigated with two types of conformations including parallel and perpendicular distributions (Figure 2). The

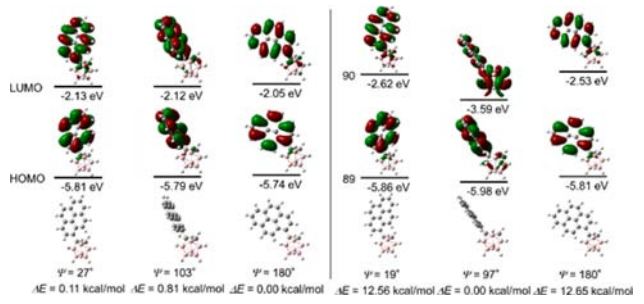

Figure 2. Calculated structure and molecular orbitals of **CBP-H** in the ground (left) and excited states. ψ values mean a dihedral angle between pyrene and the C–C bond in *o*-carborane. The differences of total energy (ΔE) and energy levels of each orbital were calculated at the B3LYP/6-31G(d) level by DFT and the B3LYP/6-31+G(d) level by TD-DFT.

difference between them was represented as the dihedral angle (ψ) between the pyrene moiety and the C–C bond in *o*-carborane. In the parallel distribution, it was shown that both the highest occupied molecular orbital (HOMO) and the lowest unoccupied molecular orbital (LUMO) were localized at the pyrene moiety. In contrast, LUMO in the perpendicular distribution was delocalized over the whole molecule through

DOI: 10.1021/acs.orglett.6b01920
Org. Lett. 2016, 18, 4064–4067

$\sigma^*-\pi^*$ conjugation. Therefore, the LE and ICT states were attributable to the parallel and perpendicular distributions, respectively. Next, the energy levels of each state were calculated (Table S1). Five hydrogens on the *o*-carborane moiety are located around the pyrene-connecting bond. Therefore, the pyrene moiety should have the steric repulsion with these hydrogens. Hence, it is difficult to have completely planar and perpendicular conformations (0° and 90°) toward the C−C bond in the *o*-carborane. Indeed, in the ground state, the parallel distributions (ψ = 26.6° and 180.0°) were energetically more stable than the perpendicular distribution (ψ = 103.4°). In contrary, the perpendicular distribution (ψ = 97.3°) was much favorable compared to the parallel distributions (ψ = 19.3° or 179.9°) in the excited state. From these data, the TICT process should be responsible for the emission of the *o*-carborane−pyrene dyads.

Next, solid-state emission properties of **CBP-H** were evaluated. To the solution of THF was added water (water/THF v/v = 99/1), and the change in emission intensity was monitored (Figure 1c, Table 1). Apparently, white turbidity

Table 1. Summary of Emission Properties of the Dyads

	THF		water		crystal	
R	λ_{em} (nm)	Φ_{PL}[a]	λ_{em} (nm)	Φ_{PL}[a]	λ_{em} (nm)	Φ_{PL}[a]
H	401, 631	0.16	596	0.40	618	0.80
Me	611	0.41	584	0.60	545	0.99
TMS	401, 632	0.19	599	0.73	579	0.99

[a]Determined as an absolute value with an integration sphere.

appeared, indicating the formation of the aggregation. Correspondingly, the intense broad emission band around 600 nm attributable to the TICT emission was obtained with the larger emission efficiency. Moreover, the large emission efficiency was observed from the crystalline sample prepared by recrystallization than those from the aggregation as well as the THF solution. These data involve two significant issues. According to the larger values of emission efficiencies in both aggregation and crystalline samples than that in the solution, it is clearly indicated that **CBP-H** possesses not only AIEE but also CIEE properties.[6a,14] Furthermore, it was suggested that **CBP-H** should be capable of presenting the TICT emission in the solid state. In the PL spectrum of the crystalline sample with **CBP-H** at 77 K (Figure S14), new emission bands were detected with the peaks around 400 and 450 nm. In particular, the emission band around 400 and 450 nm can be assigned to emissions from the LE state and the excimer as observed in the solution at 77 K, respectively. These results demonstrate that **CBP-H** can provide significant emission from the TICT state. In other words, the intramolecular rotation at the *o*-carborane moiety can be preserved even in the crystalline state. Because of the sphere structural feature of *o*-carborane, the ACQ should be suppressed. As a result, solid-state emission can be obtained via the TICT transition. The emission band around 450 nm which appeared in the water suspension could be originated from the excimer. It is likely that pyrene moieties should be condensed, leading to the excimer formation.

Based on the solid-state TICT emission from **CBP-H**, **CBP-Me** and **CBP-TMS** were designed for further enhancement to the solid-state emission efficiencies. The substituent at another carbon atom in *o*-carborane can effectively inhibit rotation at the pyrene unit. Therefore, much stronger emission could be expected from the crystalline samples. To confirm the validity of this idea, **CBP-Me** and **CBP-TMS** with strong emissions (Figures S22 and S23) were synthesized by the conversion from the lithiated **CBP-H** with methyl iodide and trimethylsilyl chloride, respectively (Scheme 1). Similarly to **CBP-H**, the characterizations of the products were executed with ^{1}H, ^{11}B, and ^{13}C NMR spectroscopies, mass measurements, and elemental analyses. The products presented good stability toward air and light under ambient conditions. Thus, we concluded that the desired dyads can be obtained.

From the PL measurements in the crystalline state, the broad emission bands were observed in the regions similar to that of the TICT emission of **CBP-H** (Figures S15 and S16). It should be emphasized that both dyads showed extremely high quantum efficiencies (Φ_{PL} > 0.99) in the crystal state (Table 1). From the PL spectra at 77 K, contrary to **CBP-H**, **CBP-Me** and **CBP-TMS** presented not vibrational emission bands but broad large ones attributable to the ICT emissions at 547 and 578 nm, respectively (Figures S17 and S18). It is likely that the intramolecular rotation should be prohibited because of steric hindrances of the substituents in *o*-carborane. The corresponding energy levels were obtained from the computer calculations (Figures S19 and S20). From these data, it can be said that *o*-carborane should be a versatile "element-block" not only for realizing multifunctional materials but also for designing highly efficient solid-state luminescent dyes.

It should be mentioned that the *o*-carborane dyads demonstrated luminescent chromism toward various external stimuli. Solvatochromic luminescence was induced owing to both the intrinsic sensitivity of the ICT state to the environmental polarity and the intensity ratios between the LE and ICT emissions.[11] **CBP-H** presented clear thermochromism by cooling. By regulating the rotation efficiency of the *o*-carborane moiety by temperature changes, the intensity ratio between the LE and TICT emissions can be tuned, leading to luminescent chromism. Finally, phase transition induced luminescent chromism with the *o*-carborane dyads. By aggregation and crystallization, the peak shifts of the emission bands were observed. In the condensed state, the molecules should be placed under hydrophobic conditions, and then the blue shifts of the ICT emission from each *o*-carborane dyad could be obtained by phase changes.

In conclusion, we present the validity of the *o*-carborane unit for constructing multifunctional emissive materials. On the basis of variable degrees of electronic interaction between *o*-carborane and pyrene depending on the dihedral angle, bright ICT was observed. From the solution sample, it was also proposed that the intramolecular rotation could be disturbed in the excited state, leading to the dual-emissive property. Additionally, it was shown that because of the sphere structural feature of *o*-carborane, the molecular rotation can proceed even in the solid state. Then AIEE and CIEE were obtained. Moreover, ACQ could be efficiently suppressed. As a result, the solid-state emission was observed. Finally, in this study, by significantly suppressing the molecular rotation in the dyads with large substituents, an extremely highly efficient solid-state emission could be detected. From these data, we can say that *o*-carborane-based dyads should be facile "element block" advance emission devices and bioprobes.

DOI: 10.1021/acs.orglett.6b01920
Org. Lett. 2016, 18, 4064−4067

■ ASSOCIATED CONTENT

Supporting Information

The Supporting Information is available free of charge on the ACS Publications website at DOI: 10.1021/acs.orglett.6b01920.

Synthetic procedures, NMR data, optical spectra, and calculation results (PDF)

■ AUTHOR INFORMATION

Corresponding Authors

*E-mail: kazuo123@chujo.synchem.kyoto-u.ac.jp.
*E-mail: chujo@chujo.synchem.kyoto-u.ac.jp.

Notes

The authors declare no competing financial interest.

■ ACKNOWLEDGMENTS

This work was partially supported by a Grant-in-Aid for Scientific Research on Innovative Areas "New Polymeric Materials Based on Element-Blocks (No.2401)" (JSPS KAKENHI Grant No. JP24102013).

■ REFERENCES

(1) (a) Luo, J.; Xie, Z.; Lam, J. W. Y.; Cheng, L.; Chen, H.; Qiu, C.; Kwok, H. S.; Zhan, X.; Liu, Y.; Zhu, D.; Tang, B. Z. *Chem. Commun.* **2001**, 1740. (b) Tong, H.; Hong, Y.; Dong, Y.; Häußler, M.; Lam, J. W. Y.; Li, Z.; Guo, Z.; Guo, Z.; Tang, B. Z. *Chem. Commun.* **2006**, 3705. (c) An, B.-K.; Kwon, S.-K.; Jung, S.-D.; Park, S. Y. *J. Am. Chem. Soc.* **2002**, *124*, 14410.

(2) (a) Yoshii, R.; Nagai, A.; Tanaka, K.; Chujo, Y. *Chem. - Eur. J.* **2013**, *19*, 4506. (b) Kumbhar, H. S.; Deshpande, S. S.; Shankarling, G. S. *Dyes Pigm.* **2016**, *127*, 161. (c) Liu, Q.; Wang, X.; Yan, H.; Wu, Y.; Li, Z.; Gong, S.; Liu, P.; Liu, Z. *J. Mater. Chem. C* **2015**, *3*, 2953. (d) Kubota, Y.; Kasatani, K.; Takai, H.; Funabiki, K.; Matsui, M. *Dalton Trans.* **2015**, *44*, 3326. (e) Wang, X.; Wu, Y.; Liu, Q.; Li, Z.; Yan, H.; Ji, C.; Duan, J.; Liu, Z. *Chem. Commun.* **2015**, *51*, 784. (f) Zheng, J.; Huang, F.; Li, Y.; Xu, T.; Xu, H.; Jia, J.; Ye, Q.; Gao, J. *Dyes Pigm.* **2015**, *113*, 502. (g) Mukherjee, S.; Thilagar, P. *Chem. - Eur. J.* **2014**, *20*, 9052. (h) Li, Z.; Lv, X.; Chen, Y.; Fu, W.-F. *Dyes Pigm.* **2014**, *105*, 157. (i) Perumal, K.; Garg, J. A.; Blacque, O.; Saiganesh, R.; Kabilan, S.; Balasubramanian, K. K.; Venkatesan, K. *Chem. - Asian J.* **2012**, *7*, 2670. (i) Quan, L.; Chen, Y.; Lv, X.-J.; Fu, W.-F. *Chem. - Eur. J.* **2012**, *18*, 14599.

(3) (a) Yoshii, R.; Suenaga, K.; Tanaka, K.; Chujo, Y. *Chem. - Eur. J.* **2015**, *21*, 7231. (b) Butler, T.; Morris, W. A.; Samonina-Kosicka, J.; Fraser, C. L. *ACS Appl. Mater. Interfaces* **2016**, *8*, 1242. (c) Wu, D.; Shao, L.; Li, Y.; Hu, Q.; Huang, F.; Yu, G.; Tang, G. *Chem. Commun.* **2016**, *52*, 541. (d) Shimizu, S.; Murayama, A.; Haruyama, T.; Iino, T.; Mori, S.; Furuta, H.; Kobayashi, N. *Chem. - Eur. J.* **2015**, *21*, 12996. (e) Dai, C.; Yang, D.; Zhang, W.; Fu, X.; Chen, Q.; Zhu, C.; Cheng, Y.; Wang, L. *J. Mater. Chem. B* **2015**, *3*, 7030. (f) Gong, S.; Liu, Q.; Wang, X.; Xia, B.; Liu, Z.; He, W. *Dalton Trans.* **2015**, *44*, 14063. (g) Fu, Y.; Qiu, F.; Zhang, F.; Mai, Y.; Wang, Y.; Fu, S.; Tang, R.; Zhuang, X.; Feng, X. *Chem. Commun.* **2015**, *51*, 5298. (h) Butler, W. A.; Morris, T.; Samonina-Kosicka, J.; Fraser, C. L. *Chem. Commun.* **2015**, *51*, 3359. (i) Wang, L.; Zhang, Z.; Cheng, X.; Ye, K.; Li, F.; Wang, Y.; Zhang, H. *J. Mater. Chem. C* **2015**, *3*, 499. (j) Yan, W.; Long, G.; Yang, X.; Chen, Y. *New J. Chem.* **2014**, *38*, 6088.

(4) Chujo, Y.; Tanaka, K. *Bull. Chem. Soc. Jpn.* **2015**, *88*, 633.

(5) (a) Peterson, J. J.; Werre, M.; Simon, Y. C.; Coughlin, E. B.; Carter, K. R. *Macromolecules* **2009**, *42*, 8594. (b) Lerouge, F.; Ferrer-Ugalde, A.; Viñas, C.; Teixidor, F.; Sillanpää, R.; Abreu, A.; Xochitiotzi, E.; Farfán, N.; Santillan, R.; Núñez, R. *Dalton Trans.* **2011**, *40*, 7541. (c) Dash, B. P.; Satapathy, R.; Gaillard, E. R.; Norton, K. M.; Maguire, J. A.; Chug, N.; Hosmane, N. S. *Inorg. Chem.* **2011**, *50*, 5485. (d) Wee, K.-R.; Han, W.-S.; Cho, D. W.; Kwon, S.; Pac, C.; Kang, S. O. *Angew. Chem., Int. Ed.* **2012**, *51*, 2677. (e) Harder, R. A.; MacBride, J. A. H.; Rivers, G. P.; Yufit, D.; Goeta, A. E.; Howard, J. A. K.; Wade, K.; Fox, M. A. *Tetrahedron* **2014**, *70*, 5182. (f) Kahlert, J.; Stammler, H.-G.; Neumann, B.; Harder, R. A.; Weber, L.; Fox, M. A. *Angew. Chem., Int. Ed.* **2014**, *53*, 3702. (g) Mukherjee, S.; Thilagar, P. *Chem. Commun.* **2016**, *52*, 1070.

(6) (a) Kokado, K.; Chujo, Y. *Macromolecules* **2009**, *42*, 1418. (b) Naito, H.; Morisaki, Y.; Chujo, Y. *Angew. Chem., Int. Ed.* **2015**, *54*, 5084. (c) Tominaga, M.; Naito, H.; Morisaki, Y.; Chujo, Y. *New J. Chem.* **2014**, *38*, 5686. (d) Tominaga, M.; Naito, H.; Morisaki, Y.; Chujo, Y. *Asian J. Org. Chem.* **2014**, *3*, 624. (e) Inagi, S.; Hosoi, K.; Kubo, T.; Shida, N.; Fuchigami, T. *Electrochemistry* **2013**, *81*, 368. (f) Kokado, K.; Nagai, A.; Chujo, Y. *Tetrahedron Lett.* **2011**, *52*, 293. (g) Kokado, K.; Nagai, A.; Chujo, Y. *Macromolecules* **2010**, *43*, 6463. (h) Bae, H. J.; Kim, H.; Lee, K. M.; Kim, T.; Lee, Y. S.; Do, Y.; Lee, M. H. *Dalton Trans.* **2014**, *43*, 4978. (i) Choi, B. H.; Lee, J. H.; Hwang, H.; Lee, K. M.; Park, M. H. *Organometallics* **2016**, *35*, 1771.

(7) (a) Tsuboya, N.; Lamrani, M.; Hamasaki, R.; Ito, M.; Mitsuishi, M.; Miyashita, T.; Yamamoto, Y. *J. Mater. Chem.* **2002**, *12*, 2701. (b) Huh, J. O.; Kim, H.; Lee, K. M.; Lee, Y. S.; Do, Y.; Lee, M. H. *Chem. Commun.* **2010**, *46*, 1138. (c) Lee, K. M.; Huh, J. O.; Kim, T.; Do, Y.; Lee, M. H. *Dalton Trans.* **2011**, *40*, 11758.

(8) (a) Kokado, K.; Chujo, Y. *Dalton Trans.* **2011**, *40*, 1919. (b) Kokado, K.; Chujo, Y. *J. Org. Chem.* **2011**, *76*, 316. (c) Boyd, L. A.; Clegg, W.; Copley, R. C. B.; Davidson, M. G.; Fox, M. A.; Hibbert, T. G.; Howard, J. A. K.; Mackinnon, A.; Peace, R. J.; Wade, K. *Dalton Trans.* **2004**, 2786. (d) Kwon, S.; Wee, K.-R.; Cho, Y.-J.; Kang, S. O. *Chem. - Eur. J.* **2014**, *20*, 5953.

(9) (a) Weber, L.; Kahlert, J.; Brockhinke, R.; Böhling, L.; Brockhinke, A.; Stammler, J.-G.; Neumann, B.; Harder, R. A.; Fox, M. A. *Chem. - Eur. J.* **2012**, *18*, 8347. (b) Kim, S.-Y.; Lee, A.-R.; Jin, G. F.; Cho, Y.-J.; Son, H.-J.; Han, W.-S.; Kang, S. O. *J. Org. Chem.* **2015**, *80*, 4573. (c) Weber, L.; Kahlert, J.; Böhling, L.; Brockhinke, A.; Stammler, H. G.; Neumann, B.; Harder, R. A.; Low, P. J.; Fox, M. A. *Dalton. Trans.* **2013**, *42*, 2266. (d) Weber, L.; Kahlert, J.; Brockhinke, R.; Böhling, L.; Halama, J.; Brockhinke, A.; Stammler, H. G.; Neumann, B.; Nervi, C.; Harder, R. A.; Low, P. J.; Fox, M. A. *Dalton. Trans.* **2013**, *42*, 10982. (e) Park, J.; Lee, Y. H.; Ryu, J. Y.; Lee, J.; Lee, M. H. *Dalton Trans.* **2016**, *45*, 5667−5675. (f) Wee, K.-R.; Cho, Y.-J.; Song, J. K.; Kang, S. O. *Angew. Chem., Int. Ed.* **2013**, *52*, 9682.

(10) Dong, H.; Wei, Y.; Zhang, W.; Wei, C.; Zhang, C.; Yao, J.; Zhao, Y. S. *J. Am. Chem. Soc.* **2016**, *138*, 1118.

(11) Valeur, B. *Molecular Fluorescence*; Wiley-VCH: Weinheim, 2002.

(12) (a) Okamoto, A.; Tainaka, K.; Nishiza, K.; Saito, I. *J. Am. Chem. Soc.* **2005**, *127*, 13128. (b) Tanaka, K.; Jeon, J.-H.; Inafuku, K.; Chujo, Y. *Bioorg. Med. Chem.* **2012**, *20*, 915.

(13) (a) Cao, C.; Liu, X.; Qiao, Q.; Zhao, M.; Yin, W.; Mao, D.; Zhang, H.; Xu, Z. *Chem. Commun.* **2014**, *50*, 15811. (b) Hu, R.; Lager, E.; Aguilar-Aguilar, A.; Liu, J.; Lam, J. W. Y.; Sung, H. H. Y.; Williams, I. D.; Zhong, Y.; Wong, K. S.; Peña-Cabrera, E.; Tang, B. Z. *J. Phys. Chem. C* **2009**, *113*, 15845. (c) Ito, A.; Ishizaka, S.; Kitamura, N. *Phys. Chem. Chem. Phys.* **2010**, *12*, 6641. (d) Grabowski, Z. R.; Rotkiewicz, K.; Rettig, W. *Chem. Rev.* **2003**, *103*, 3899.

(14) (a) Yoshii, R.; Hirose, A.; Tanaka, K.; Chujo, Y. *Chem. - Eur. J.* **2014**, *20*, 8320. (b) Yoshii, R.; Hirose, A.; Tanaka, K.; Chujo, Y. *J. Am. Chem. Soc.* **2014**, *136*, 18131.

DOI: 10.1021/acs.orglett.6b01920
Org. Lett. 2016, 18, 4064−4067